Supporting information

Colloidal Synthesis and Ultraviolet Luminescence of Rb_2AgI_3 Nanocrystals

Yuan Deng [1,†], Yicheng Zeng [1,†], Wanying Gu [1], Pan Huang [1], Geyu Jin [1], Fangze Liu [2], Jing Wei [1] and Hongbo Li [1,*]

[1] School of Materials Science and Engineering, Beijing Institute of Technology, Beijing 100081, China
[2] Advanced Research Institute of Multidisciplinary Sciences, Beijing Institute of Technology, Beijing 100081, China
* Correspondence: hongbo.li@bit.edu.cn
† These authors have contributed equally to this work.

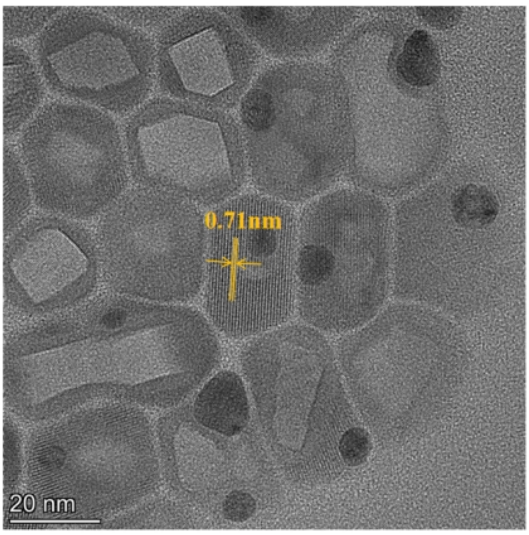

Figure S1. HRTEM image of Rb_2AgI_3 NCs.

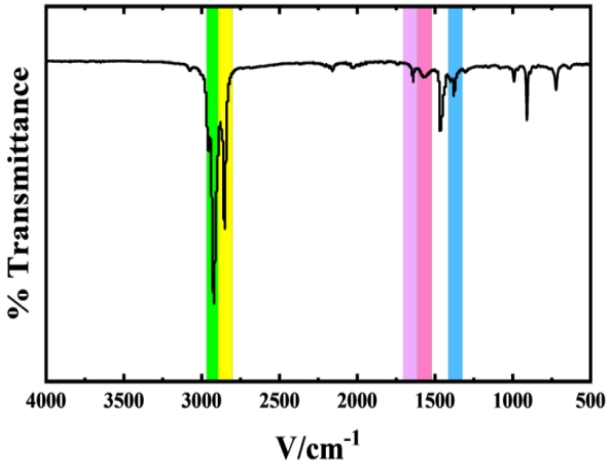

Figure S2. FTIR pattern of Rb_2AgI_3 NCs. Vibrating bands at 1650 cm^{-1} and 1380 cm^{-1} can be assigned to countersymmetric telescopic vibration and symmetrical telescopic vibration modes from oleic acid ligand $-COO^-$, respectively. Peaks around 1570 cm^{-1} indicate the bending vibration of the $-NH_2$ group N-H in oleamine. The vibration bands at 2930 cm^{-1} and 2860 cm^{-1} are attributed to the C-H bond tensile vibrations of $-CH_3$ and $-CH_2$, respectively.

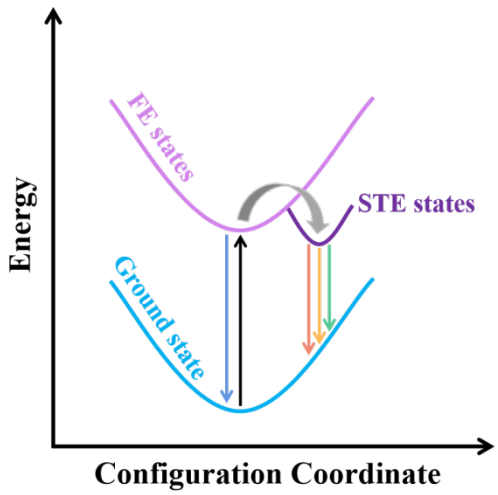

Figure S3. Schematic diagram of self-trapped exciton luminescence mechanism.

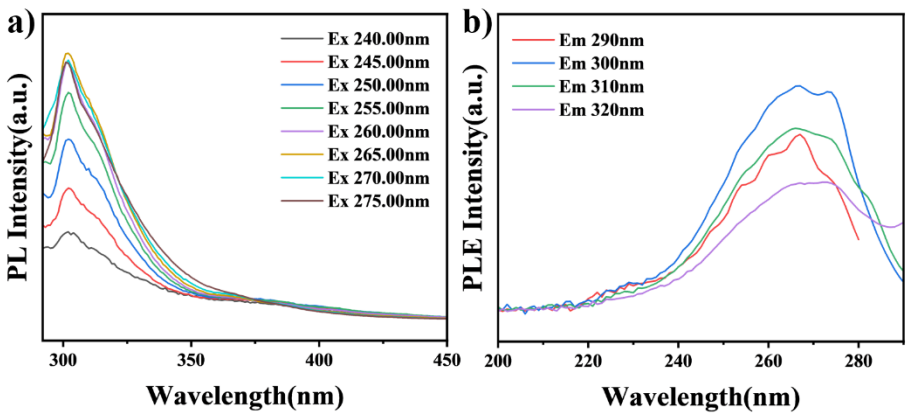

Figure S4. Wavelength-dependent (a) PL and (b) PLE spectra of Rb_2AgI_3 NCs.

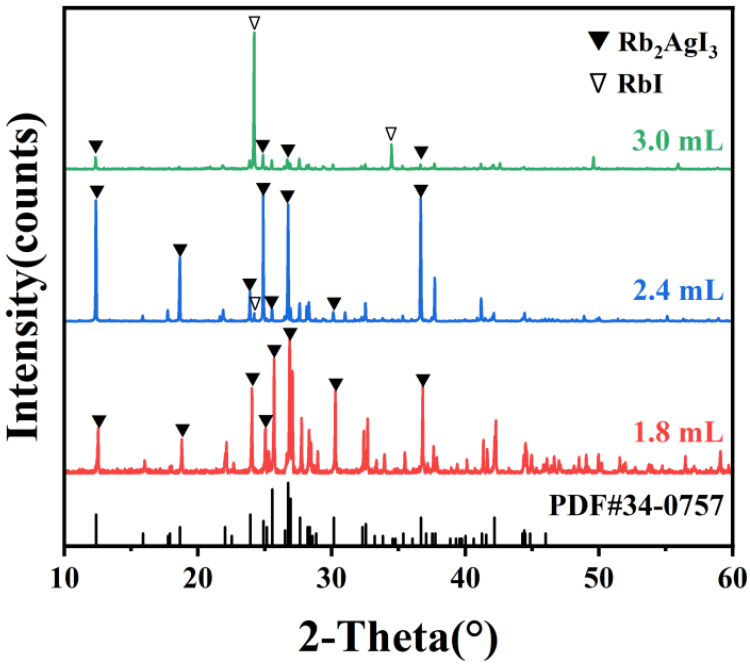

Figure S5. XRD pattern of of the product obtained by changing the amount of iodine precursor injection

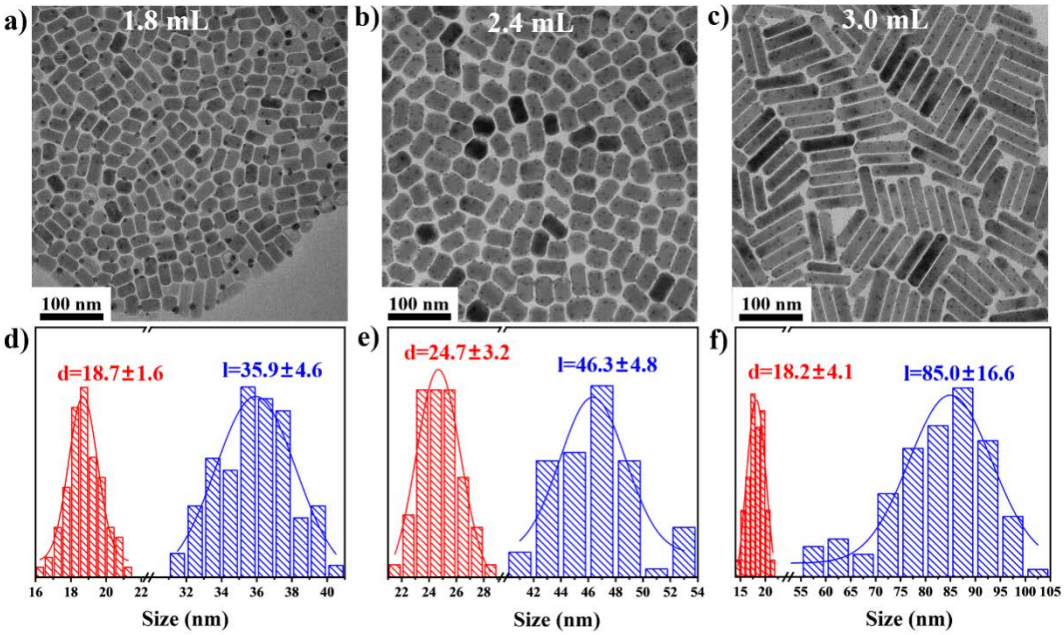

Figure S6. (a-c) TEM image and (d-f) its particle size distribution of the product obtained by changing the amount of iodine precursor injection.

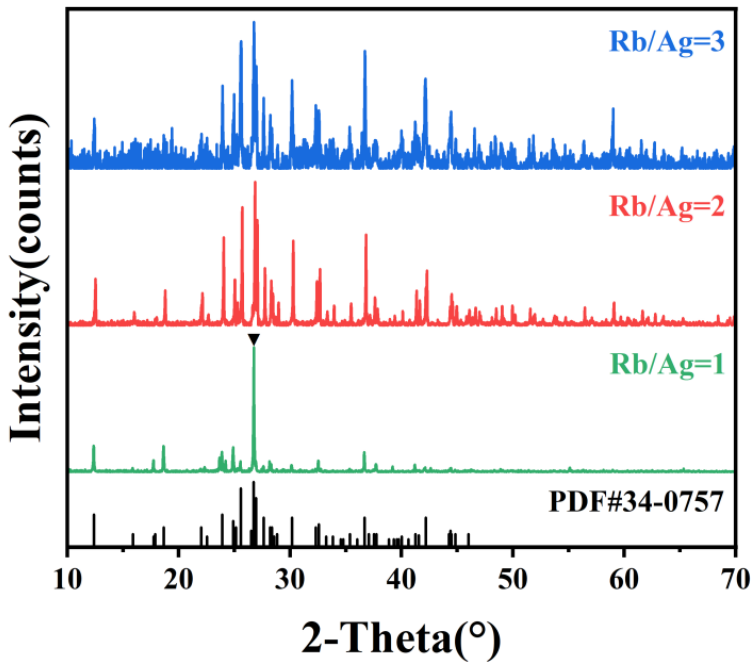

Figure S7. XRD pattern of of the product obtained obtained by changing the feeding ratio of rubidium salt and silver salt in the initial solution.

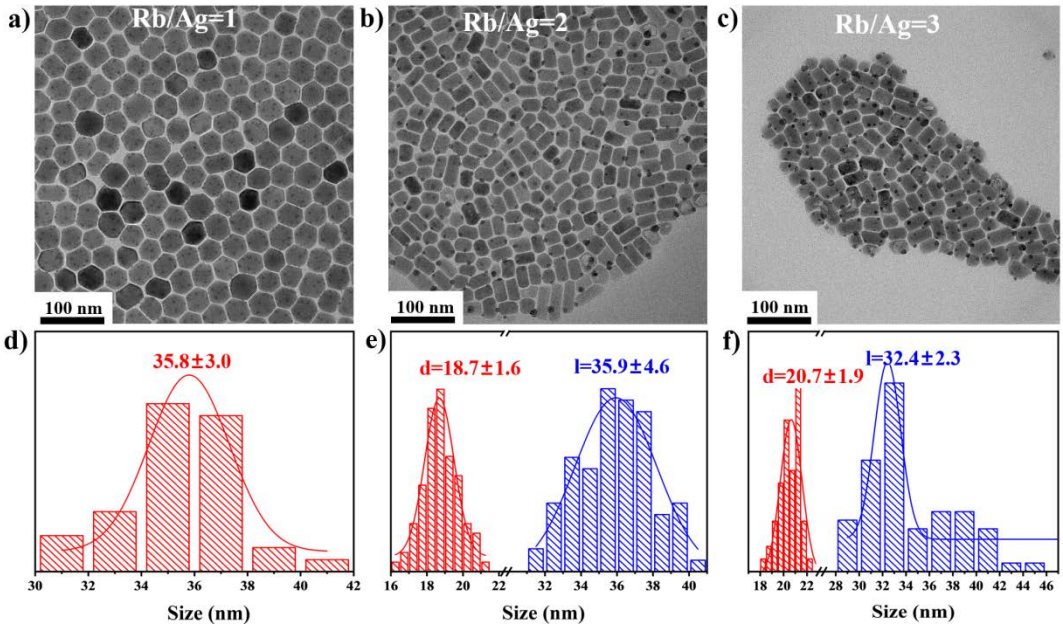

Figure S8. (a-c) TEM images and (d-f) its particle size distribution of the product obtained by changing the feeding ratio of rubidium salt and silver salt in the initial solution.

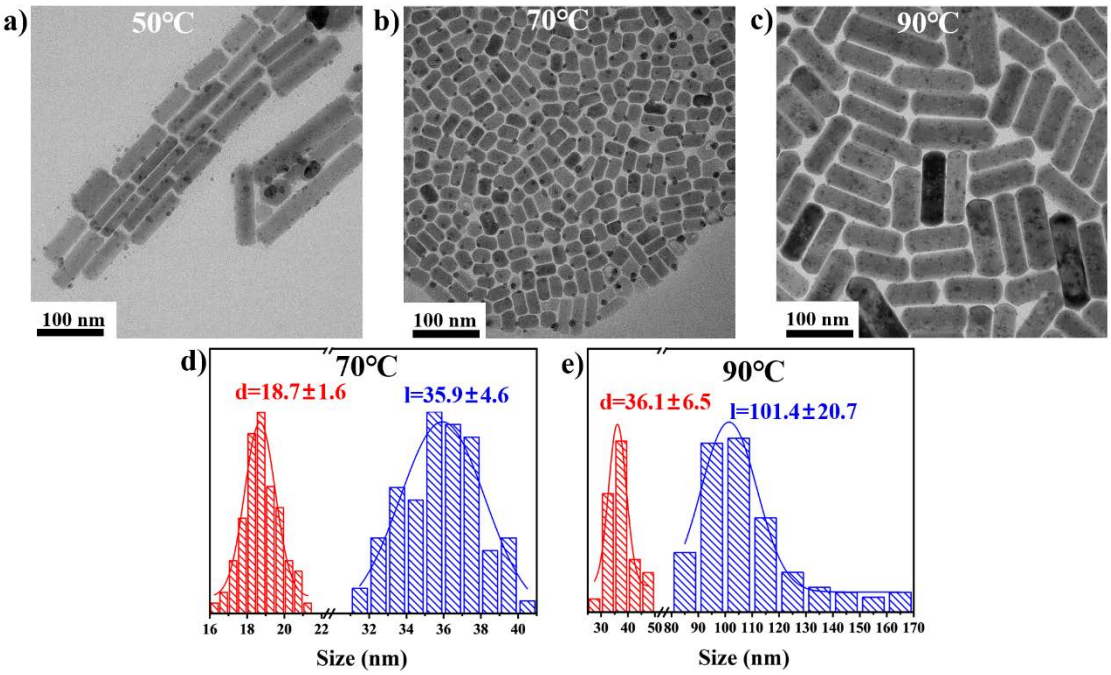

Figure S9. (a-c) TEM images and (d-e) its particle size distribution of the product obtained by changing the reaction temperature (50 °C, 70 °C, 90 °C).

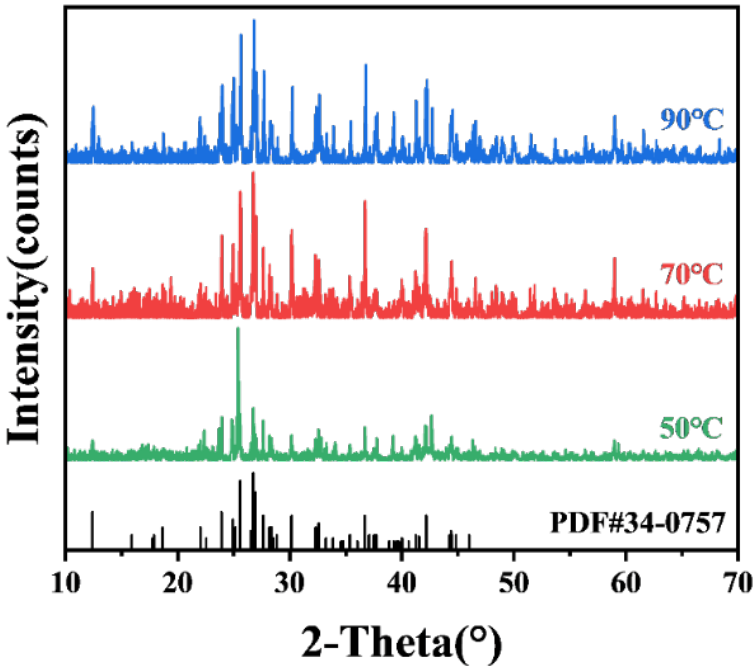

Figure S10. XRD pattern of of the product obtained obtained by changing the reaction temperature (50 °C, 70 °C, 90 °C).

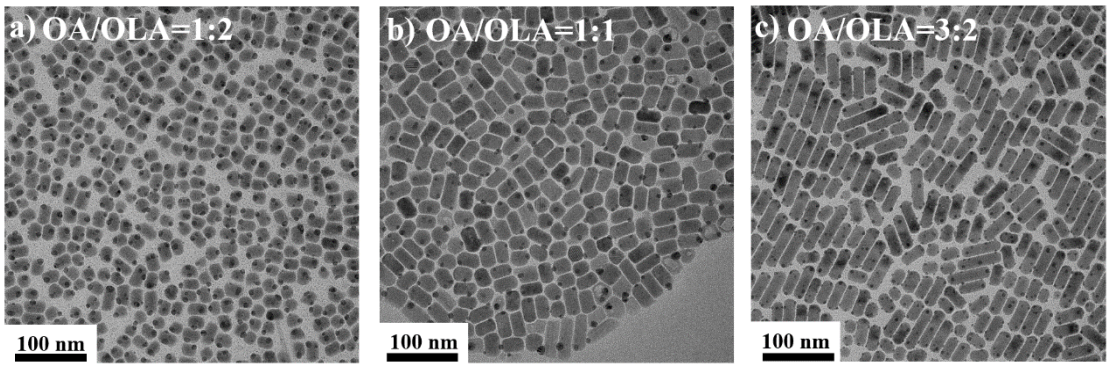

Figure S11. TEM image of the Rb_2AgI_3 NCs obtained by changing the OA/OLA ratio.

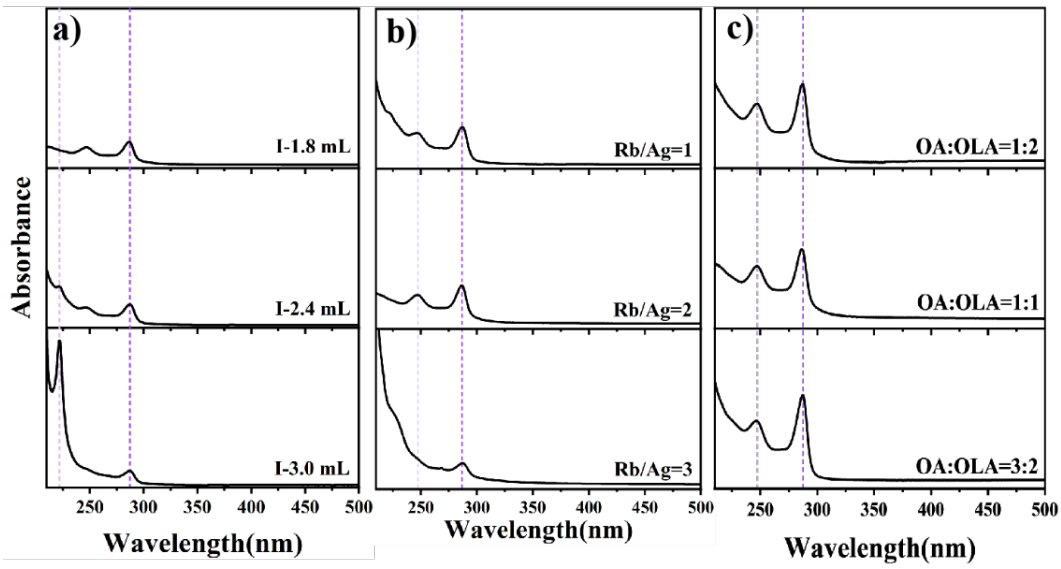

Figure S12. UV-Vis spectra of Rb_2AgI_3 NCs obtained under different reaction conditions.

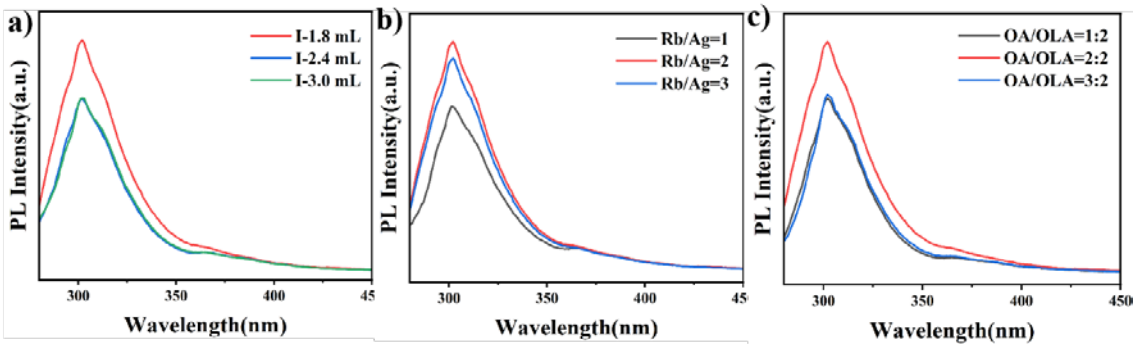

Figure S13. PL spectra of Rb_2AgI_3 NCs obtained under different reaction conditions.